

Analysis of the relevance between computed tomography characterization and pathology of pulmonary ground-glass nodules with different pathology types

Bilgisayarlı tomografi karakterizasyonu ve farklı patoloji türleri olan pulmoner buzlu cam nodüllerinin patolojisi arasındaki ilişkinin değerlendirilmesi

Zhang Youguo^{1B}, Wang Chengye^{1B}, Cheng Xiaofei^{1B}, Zhang Xuefei^{1B}, Liu Changhong^{1B}

Department of Thoracic Surgery 1, The Second Hospital of Dalian Medical University, Dalian, China

ABSTRACT

Background: In this study, we aimed to analyze the relevance between computed tomography characterization and pathology of pulmonary ground-glass nodules with different pathology types.

Methods: Between January 2017 and December 2018, a total of 657 patients (191 males, 466 females; mean age: 60.9±8.1 years; range, 34 to 80 years) with pathologically diagnosed ground-glass nodules were retrospectively analyzed. The clinicopathological characteristics and computed tomography characterizations of patients with ground-glass nodules who received surgical resection were analyzed. The clinical data including age, sex, smoking status and medical history were recorded. Computed tomography characterizations included the location and size of the tumor, the size of the consolidation components, density uniformity, shape, margin, tumor-lung interface, internal signs and surrounding signs.

Results: Based on the computed tomography imaging characteristics, a mean computed tomography value of ≥ 444.5 HU was more likely to indicate malignant lesions, while ≤ 444.5 HU indicated benign lesions. A malignant ground-glass nodules' maximum diameter of < 6.78 mm, a diameter of the consolidation component of < 3.88 mm, and a mean computed tomography value of < 536.5 HU were more likely to indicate atypical adenomatous hyperplasia and adenocarcinoma *in situ*. A maximum diameter of malignant ground-glass nodules of > 11.52 mm, a diameter of the consolidation component of > 6.20 mm, and a mean computed tomography value of ≥ 493.5 HU were more likely to indicate invasive adenocarcinomas. The focus between these parameters indicated minimally invasive adenocarcinomas.

Conclusion: Ill-defined tumor-lung interface, irregular in shape, and smooth nodule margins suggest benign lesions while round or oval, clear tumor-lung interface, spiculation signs, lobulation signs, bubble signs, air bronchograms, pleural indentations, and vessel convergences are helpful in the diagnosis of malignant lesions. A clear tumor-lung interface, the spiculation signs, lobulation signs, and bubble signs indicate the invasion of the lesions.

Keywords: Computed tomography, ground-glass nodules, lung neoplasms, pathology.

ÖZ

Amaç: Bu çalışmada bilgisayarlı tomografi özellikleri ve farklı patoloji tiplerinde akciğer buzlu cam nodüllerinin patolojisi arasındaki ilişki incelendi.

Çalışma planı: Ocak 2017 - Aralık 2018 tarihleri arasında patolojik olarak tanı konan buzlu cam nodülleri olan toplam 657 hasta (191 erkek, 466 kadın; ort. yaş: 60.9±8.1 yıl; dağılım, 34 to 80 yıl) retrospektif olarak incelendi. Cerrahi rezeksiyon yapılan buzlu cam nodülleri olan hastaların klinikopatolojik özellikleri ve bilgisayarlı tomografi özellikleri analiz edildi. Yaş, cinsiyet, sigara içme durumu ve tıbbi öykü dahil olmak üzere klinik veriler kaydedildi. Bilgisayarlı tomografi özellikleri arasında tümörün yeri ve boyutu, konsolidasyon komponentinin boyutu, dansite benzerliği, şekil, sınır, tümör-akciğer arayüzü, dahili bulgular ve çevresel bulgular yer alıyordu.

Bulgular: Bilgisayarlı tomografi görüntüleme özelliklerine göre, ≥ 444.5 HU ortalama bilgisayarlı tomografi değeri malign lezyonları gösterirken, ≤ 444.5 HU benign lezyonları gösteriyordu. < 6.78 mm'lik malign buzlu cam nodüllerinin maksimum çapı, < 3.88 mm'lik konsolidasyon komponent çapı ve < 536.5 HU'luk ortalama bilgisayarlı tomografi değeri atipik adenomatöz hiperplazi ve adenokarsinom *in situ*yu gösteriyordu. > 11.52 mm'lik malign buzlu cam nodüllerinin maksimum çapı, > 6.20 mm'lik konsolidasyon komponent çapı ve ≥ 493.5 HU'luk ortalama bilgisayarlı tomografi değeri invaziv adenokarsinomları gösteriyordu. Bu parametreler arasındaki odak, minimal invaziv adenokarsinomları gösteriyordu.

Sonuç: Belirsiz tümör-akciğer arayüzü, düzensiz şekil ve düzgün nodül sınırları iyi huylu lezyonları düşündürürken, yuvarlak veya oval, temiz tümör-akciğer arayüzü, spikülasyon bulguları, lobülasyon bulguları, kabarcık bulguları, hava bronkogramları, plevral girintiler ve damar yakınsaklıkları malign lezyonların tanısında yardımcıdır. Temiz tümör-akciğer arayüzü, spikülasyon bulguları, lobülasyon bulguları ve kabarcık bulguları lezyonların invazyonunu gösterir.

Anahtar sözcükler: Bilgisayarlı tomografi, buzlu cam nodülleri, akciğer tümörleri, patoloji.

Corresponding author: Liu Changhong.

E-mail: 17709870870@163.com

Doi: 10.5606/tgkdc.dergisi.2023.22239

Received: September 09, 2021

Accepted: November 22, 2021

Published online: January 30, 2023

Cite this article as: Youguo Z, Chengye W, Xiaofei C, Xuefei Z, Changhong L. Analysis of the relevance between computed tomography characterization and pathology of pulmonary ground-glass nodules with different pathology types. Turk Gogus Kalp Dama 2023;31(1):95-104. doi: 10.5606/tgkdc.dergisi.2023.22239.

©2023 All right reserved by the Turkish Society of Cardiovascular Surgery.



This is an open access article under the terms of the Creative Commons Attribution-NonCommercial License, which permits use, distribution and reproduction in any medium, provided the original work is properly cited and is not used for commercial purposes (<http://creativecommons.org/licenses/by-nc/4.0/>).

Pulmonary ground-glass nodules (GGNs) are defined as pulmonary nodules with a slight increase in lung tissue density in the computed tomography (CT) lung window, and the margin is clear or unclear, but vessels and bronchial texture are still visible in the lesions.^[1] A pure GGN (pGGN) was identified as a lung nodule without solid component, while a mixed GGN (mGGN) was identified as that with both ground-glass opacity (GGO) and solid. With the extensive application of low-dose thin-section chest CT scans in lung neoplasm screening, the detection rate of GGNs in the population has increased significantly in the last decade. In 2015, according to the new small five biopsy and cytological classification proposed by 2011 International Association for the Study of Lung Cancer (IASLC)/American Thoracic Society (ATS)/European Respiratory Society (ERS) classification, the World Health Organization (WHO) released a new classification of lung adenocarcinoma^[2,3] and adopted different classification methods for lung adenocarcinomas that have been pathologically diagnosed. Ground-glass nodules can be benign lesions (such as infection, inflammation, and focal fibrosis) or malignant lesions (such as lung adenocarcinoma). Pulmonary small GGNs with a diameter of less than 30 mm are difficult to diagnose by CT scan, and as the nodules are small and the density of nodules is low, needle biopsy usually fails to create a clear diagnosis of the disease. The statement on the treatment of pulmonary nodules published by Fleischner Society in 2017^[4] suggests that GGNs less than 6 mm in diameter do not need regular follow-up, but for GGNs more than 6 mm in size should be set in the treatment of nodules policy according to the diameter of the solid component. For persistency and the solid components which are greater than 6 mm nodules in diameters should be deemed to be highly suspicious.

In the present study, we aimed to analyze the relevance between CT characterization and pathology of pulmonary GGNs with different pathology types.

PATIENTS AND METHODS

This single-center, retrospective study was conducted at The Second Hospital of Dalian Medical University, Department of Thoracic Surgery between January 2017 and December 2018. Initially, nearly 4,000 lung cancer patients who underwent surgical operation were screened. A total of 657 patients (191 males, 466 females; mean age: 60.9±8.1 years; range, 34 to 80 years) with pathologically diagnosed GGNs (less than 30 mm in diameter) were enrolled. None of the patients had a history of primary malignant

tumor. The imaging data of pulmonary GGNs patients who underwent thin-section CT examination in our hospital were analyzed. All the lesions were GGNs (less than 30 mm) and were surgically resected within one month after CT scanning.

The CT used Somatom Sensation-64 (Siemens Medical System, Munich, Germany), 120 kVp, 100 mAs. All images were reconstructed with section thickness of 2 mm, lung window width 1,600 HU, window width -600 HU, mediastinal window width 350 HU, window width 35 HU. The size of nodules and its consolidation component, mean CT value, location, shape, density uniformity, margin, tumor-lung interface, internal and surrounding signs of the nodules were recorded. The size of the nodules was defined as the maximum diameter of the lesions on axial images. The diameters of the solid component were measured in the same way. The density uniformity was divided into homogeneous, less homogeneous, and heterogeneous density. It was defined as homogeneous density, when there was no bubble-like lucency in the lesion, and when there were more than three lucent areas in the lesion or the local density in the lesion was slightly higher than other parts, but did not reach the solid density, it was defined as heterogeneous density, and between the two above situations was defined as less homogeneous. Two radiologists with more than five years of experience in thoracic radiology performed CT images on both the window of the lung (window width 350 HU; window height 35 HU) and mediastinal window (window width 1600 HU; window level, -600 HU) was reviewed independently without any clinical information. They discussed with each other, when there was disagreement.

Two pathologists were blind to the patient's imaging information, re-read all the tumor sections stained with hematoxylin and eosin, and made pathological diagnosis depending on the IASLC/ATS/ERS classification. The pre-invasive lesions (including atypical adenomatous hyperplasia [AAH] and adenocarcinoma *in situ* [AIS]), minimally invasive adenocarcinoma [MIA] and invasive adenocarcinoma [IAC] were pathologically diagnosed and classified based on the 2015 edition of lung adenocarcinoma classification.^[2] In case of disagreements between the two pathologists, they reached a consensus after discussing and/or consulting with a third pathologist with a senior professional title.

Statistical analysis

Statistical analysis was performed using the IBM SPSS version 25.0 software (IBM Corp., Armonk, NY, USA). Descriptive data were expressed

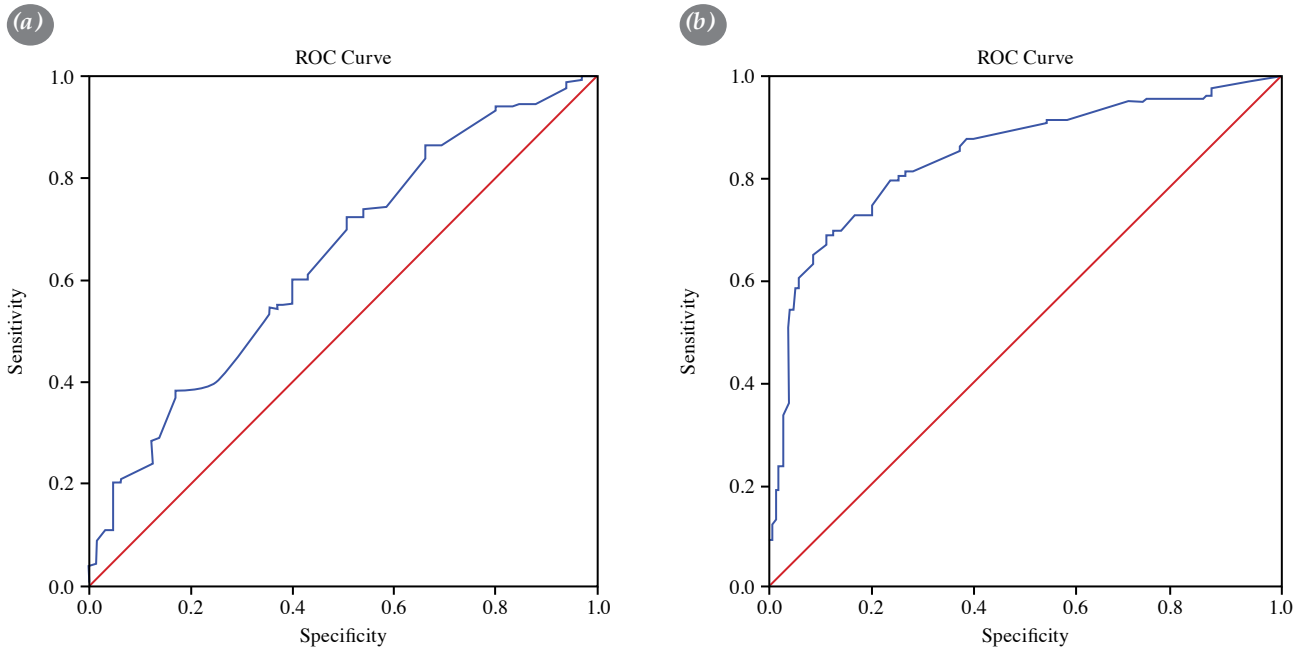


Figure 1. (a) The optimal cut-off value of lesion size in differentiating pre-invasive lesions from MIAs. **(b)** The optimal cut-off value of lesion size in differentiating MIAs from IACs.
MIAs: Minimally invasive adenocarcinomas; IACs: Invasive adenocarcinomas.

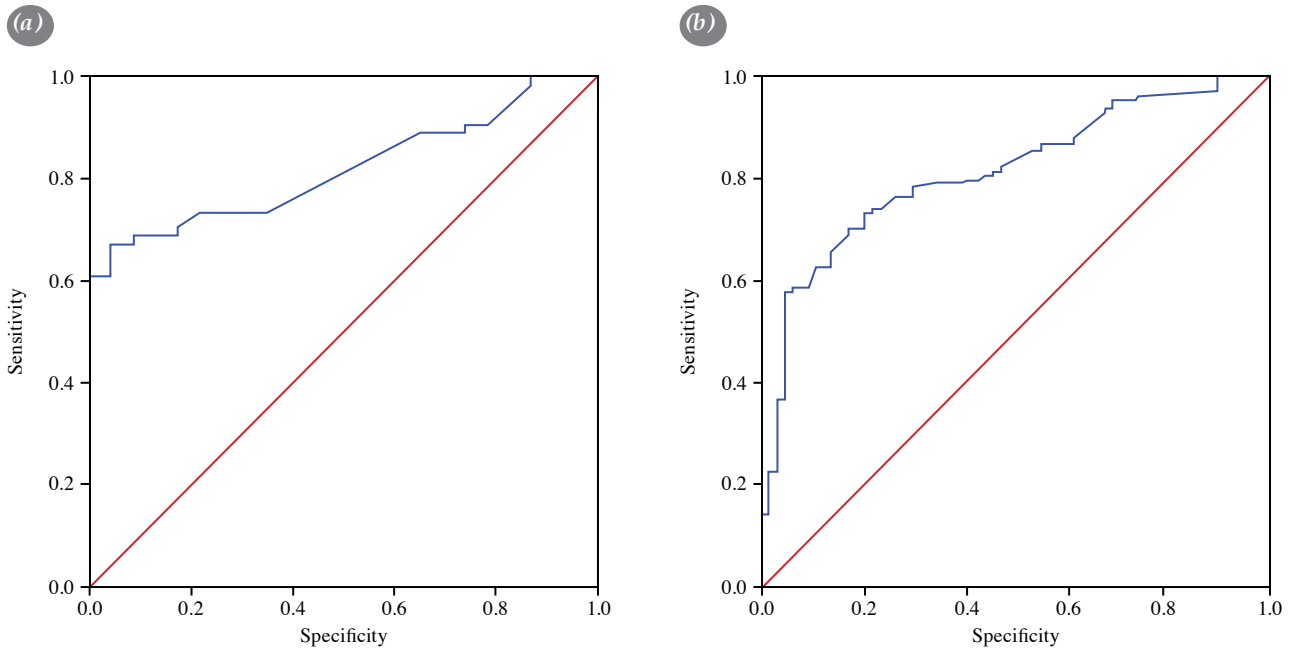


Figure 2. (a) The optimal cut-off value of consolidation component in distinguishing pre-invasive lesions from MIAs. **(b)** The optimal cut-off value of consolidation component's size in distinguishing MIAs from IACs.
MIAs: Minimally invasive adenocarcinomas; IACs: Invasive adenocarcinomas.

in mean \pm standard deviation (SD), median (min-max) or number and frequency, where applicable. One-way analysis of variance (ANOVA) was used to analyze the correlation of patients' age, nodule

size, consolidation component's size, mean CT value with histological types and invasion. According to homogeneity of variance, the Student Newman-Keuls test and Kruskal-Wallis test were used. The correlation

of patient's sex, location distribution, shape, tumoring interface, density uniformity, margin, internal and surrounding characteristics with histological types and invasion were analyzed using the Pearson chi-square test and Fisher exact test. The optimal cut-off value of lesion size, consolidation component's size and mean CT value between pre-invasive lesions and MIA and between MIA and IACs were calculated by using the receiver operating characteristic (ROC) curve. A p value of <0.05 was considered statistically significant.

RESULTS

There were no significant differences in sex and location between benign and malignant lesions. No significant difference was found in smoking status, hypertension history, diabetes history, and coronary heart disease history in each group (Table 1). However, statistically significant differences were observed among the pre-invasive group, MIA group, and IAC group. The sizes of pre-invasive lesions and MIAs were significantly smaller than that of invasive adenocarcinoma (Table 2). The diameters of malignant lesions increased with the degree of invasion of the lesion. No statistically significant differences between benign and malignant group in size were found. The optimal cut-off value of lesion size in differentiating pre-invasive lesions from MIAs was 6.78 mm (AUC=0.643; 95% confidence interval [CI]: 0.566-0.720), with 72.3% sensitivity and 49.2% specificity (Figure 1a).

The optimal cut-off value of lesion size in differentiating MIAs from IACs was 11.52 mm (AUC=0.845; 95% CI: 0.811-0.879), with 68.8% sensitivity and 89.1% specificity (Figure 1b). Significant differences in the diameters of the consolidation components were observed among pre-invasive lesions, MIA and IAC groups, although it did not significantly differ between benign and malignant lesions. The optimal cut-off value of consolidation component in distinguishing pre-invasive lesions from MIAs was 3.88 mm in size (AUC=0.819; 95% CI: 0.734-0.905), with 67.2% sensitivity and 95.7% specificity Figure 2a, and that of consolidation component was 6.2 mm in distinguishing MIAs from IACs (AUC=0.809; 95% CI: 0.756-0.853), with 73% sensitivity and 79.7% specificity (Figure 2b).

The optimal cut-off value of mean CT value between the benign nodules and malignant nodules was -444.5 HU (AUC=0.621; 95% CI: 0.542-0.699) with sensitivity of 58.8% and specificity of 67.7%, respectively (Figure 3a). Significant differences

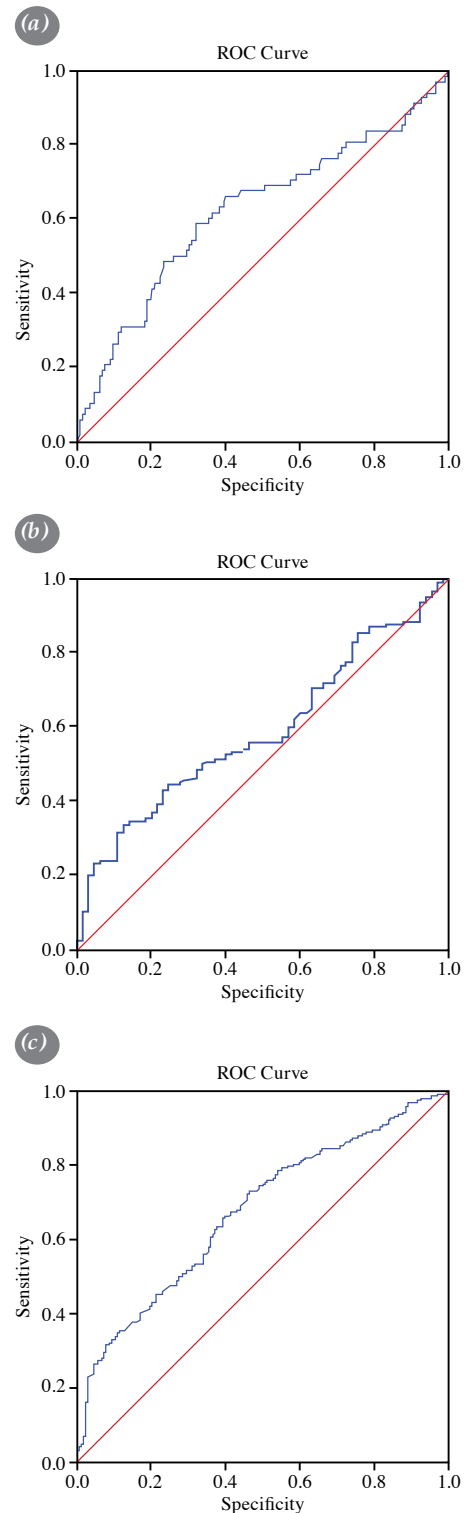


Figure 3. (a) The optimal cut-off value of mean CT value between the benign lesions and malignant lesions. (b) The optimal cut-off value of mean CT value between the pre-invasive lesions and MIA. (c) The optimal cut-off value of mean CT value between the MIA lesions and IAC lesions.

CT: Computed tomography; MIAs: Minimally invasive adenocarcinomas; IACs: Invasive adenocarcinomas.

were also found among the pre-invasive lesions, MIAs, and IACs. The optimal cut-off value between the pre-invasive lesions and MIAs was -493.5 HU (AUC=0.589; 95% CI: 0.514-0.664) (Figure 3b), and that between the MIA lesions and IAC lesions was -536.5 HU (AUC=0.675; 95% CI: 0.628-0.721) (Figure 3c). Significant differences were found between benign lesions and malignant lesions.

There were statistically significant differences between benign lesions and malignant lesions in morphological characteristics of lesions regarding the shape, tumor-lung interface, margin, internal signs and pleural indentation (Table 3). The malignant nodules manifested a round or oval shape to a greater extent than benign nodules. The tumor-lung interface was significantly different among the four groups.

The proportion of malignant nodules with ill-defined tumor-lung interface was significantly higher than that of benign GGNs.

There were statistically significant differences in the margin among the benign and each malignant group. There were also statistically significant differences between the benign group and malignant group and among the three malignant lesion groups. The malignant nodules displayed a spiculation sign to a greater extent than benign nodules and in the IAC nodules there were more than pre-invasive lesions and MIAs. Significant differences in the lobulation sign were also observed among the four groups. The malignant lesions showed more lobulated margins, while the benign lesions appeared as a smoother margin than malignant lesions.

Table 1. Clinical characteristics of patients

Clinical characteristics	Pathologic group		<i>p</i>
	Benign lesions (n=68)	Malignant lesions (n=589)	
	n	n	
Age (year)			0.153
<60 years-old	33	231	
≥60 years-old	35	358	
Sex			0.179
Male	15	176	
Female	53	413	
Smoking status			0.155
Yes	13	80	
No	55	509	
Previous history			
Hypertension history			0.559
Yes	15	149	
No	53	440	
Diabetes history			0.689
Yes	7	52	
No	61	537	
Coronary heart disease			
History			0.791
Yes	2	21	
No	66	568	
Location			0.087
LUL	10	154	
LLL	12	89	
RUL	23	217	
RML	5	38	
RLL	18	91	

LUL: Left upper lobe; LLL: Left lower lobe; RUL: Right upper lobe; RML: Right middle lobe; RLL: Right lower lobe.

Table 2. Patients with lung nodules on CT parameters

	Pathologic group											
	Benign lesions		Pre-invasive lesions		MIA lesions		IAC lesions					
	Mean±SD		Mean±SD		Mean±SD		Mean±SD					
Mean diameters (mm)	11.1±7.2		6.8±2.4		8.5±3.7		16.1±6.8		p1	p2	p3	p4
The mean diameter of the consolidation components (mm)	7.9±2.5		2.7±0.9		5.2±2.7		10.4±5.7		0.06	0.042	0.000	0.000
The mean CT value (HU)	-425.6±202.1		-606.3±101.2		559.4±138.5		455.1±175.9		0.278	0.046	0.000	0.000

CT: Computed tomography; SD: Standard deviation; MIA: Minimally invasive adenocarcinoma; IAC: Invasive adenocarcinoma; p1: The statistical difference between the benign group and the malignant group; p2: The statistical difference between the pre-invasion group and the MIA group; p3: The statistical difference between the pre-invasion group and the IAC group; p4: The statistical difference between the MIA group and the IAC group.

The malignant nodules showed a greater degree than benign nodules in bubble signs. With the increase of the proportion of the degree of invasion of lesions, the bubble sign appeared increasingly high. Malignant lesions displayed a greater extent of air bronchogram than benign nodules, the IACs also displayed a greater extent to pre-invasive lesions and MIAs. However, there were no statistically significant differences between pre-invasive lesions and MIAs.

There were significant differences in pleural indentation between benign lesions and malignant lesions, pleural indentation is more frequent in malignant nodules than benign nodules. In vessel convergence, significant differences were observed between benign lesions and malignant lesions, and it appeared more frequently in malignant lesions than benign lesions.

The density uniformity of lesions between the benign and malignant groups did not show significant differences. There were also no statistically significant differences in patients' sex and lesion location between benign and malignant lesions. No statistically significant differences in smoking history and previous history were observed in each group, either.

The lesion size, shape, tumor-lung interface, smooth margin, spiculation signs, lobulation signs, bubble signs, air bronchogram signs, pleural indentation signs and vessel convergence signs, solid component diameters, mean CT value of lesions as independent variables, malignant lesions were dependent variables. Binary logistics regression analysis revealed that lesion shapes, bubble signs, air bronchogram signs, pleural indentation signs and vessel convergence signs, the mean CT value of lesions were related to malignant lesions (p<0.05). The AUC of malignant pulmonary nodules with an average CT value of -444.5 HU was 0.621 (95% CI: 0.542-0.699).

DISCUSSION

Different pathological types of GGNs have different treatment methods and prognosis. Low-dose chest CT examination is the main method for screening and diagnosing GGN currently.^[5] Therefore, the CT characteristics used to distinguish benign and malignant lesions that acted as GGNs on chest CT were the most crucial consequences of the current study. This discovery may help surgeons to choose better treatments for GGN.

According to the results of previous studies, nodules larger than 30 mm in size should be considered

Table 3. Morphological characteristics of GGNs

Morphologic characteristics	Pathologic group												p1	p2	p3	p4				
	Benign lesions (n=68)				Pre-invasive lesions (n=65)				MIA lesions (n=184)								IAC lesions (n=339)			
	n	%	n	%	n	%	n	%	n	%	n	%					n	%		
Shape																				
Round or oval	32	47.06	45	69.23	139	75.54	181	53.24	0.000	0.319	0.017	0.000	0.000							
Irregular	36	52.94	20	30.77	45	24.46	159	46.76												
Density uniformity																				
Homogeneous	28	41.18	36	55.38	90	48.91	57	16.76	0.109	0.323	0.000	0.000								
Less homogeneous	6	8.82	9	13.85	25	13.59	24	7.06												
Heterogeneous	34	52.31	20	30.77	69	37.5	259	76.18												
Tumor-lung interface																				
Well-defined	43	63.24	15	23.08	89	48.37	211	62.06	0.000	0.000	0.000	0.002								
Ill-defined	25	36.76	50	76.92	95	51.63	129	36.47												
Margin																				
Smooth	31	45.59	47	72.31	96	52.17	103	30.29	0.000	0.005	0.000	0.000								
Spiculation sign	16	23.53	5	7.69	33	17.93	124	36.47	0.000	0.048	0.000	0.000								
Lobulation sign	19	27.94	7	10.77	48	26.09	133	39.12	0.000	0.010	0.000	0.003								
Internal signs																				
Bubble sign	5	7.35	14	21.54	68	36.96	162	47.65	0.000	0.023	0.000	0.019								
Air bronchogram	5	7.35	14	21.54	34	27.17	119	35	0.000	0.591	0.034	0.000								
Surrounding signs																				
Pleural indentation	4	5.89	12	18.46	50	27.17	138	40.59	0.000	0.163	0.001	0.002								
Vessel convergence	2	2.94	8	12.31	20	10.87	60	17.65	0.006	0.752	0.291	0.039								

GGNs: Pulmonary ground-glass nodules; MIA: Minimally invasive adenocarcinoma; IAC: Invasive adenocarcinoma; p1: The statistical difference between the benign group and the malignant group; p2: The statistical difference between the pre-invasion group and the MIA group; p3: The statistical difference between the pre-invasion group and the IAC group; p4: The statistical difference between the MIA group and the IAC group; p<0.05 is considered statistically difference.

malignant unless other evidence can prove it, as the literature suggests that the probability of these nodules being malignant is close to 93 to 97%.^[6] The study of Lee et al.^[7] showed that the optimal cut-off value of nodular diameter for pure GGN was 8 mm, and the optimal critical value for mixed GGN was 16 mm. However, we found no significant differences in the lesions' sizes between benign and malignant groups. This may be related to the small number of benign nodules resected by surgical operation that we collected. However, the size of malignant nodules was closely related to the degree of invasion of the lesions: the higher the degree of invasion of the lesions, the larger its diameter. Otherwise, we found that the size of the solid components of the lesions may predict the degree of invasion of malignant nodules more accurately than the whole lesion size. Ge et al.^[8] measured lesion size, proportion of GGO composition and long diameters and size of consolidation components on CT to establish the CT diagnostic standard of pulmonary GGNs. Through the ROC curve, lesion size, the diameter of solid components, the proportion of GGO components among each had an important relationship with pathological types of lesions. Among them, the diameters of the solid component of the lesion and the proportion of the GGO component had a higher diagnostic value with an AUC of >0.90. In addition, Shengli et al.^[9] compared 216 high-resolution CT characteristics and measurements for prediction of lesions' invasion in mGGNs. They found that the greater the diameter of the consolidation component (odds ratio [OR]: 337.004, 95% CI: 17.431-6 515.57, $p < 0.001$), the mGGNs were more likely to be pathologically confirmed as IAC. Our study results are similar to them.

Previous studies^[10] have shown that the mean CT value of lesions can be used as a method to distinguish different pathological types of lung adenocarcinoma. Our study showed statistically significant differences in the mean CT value in the malignant groups. The mean CT value of IAC lesions was higher than that of pre-invasive lesions and MIAs. The study findings of Weijie et al.^[11] are consistent with our findings.

As for the morphological CT features, there were significant differences between benign lesions and malignant lesions of lesion shapes in our study. It showed that the proportion of round or oval in malignant lesions (365/589, 61.97%) was significantly higher than that of benign nodules (32/68, 47.06%), which is similar to the findings of Gao et al.^[12] We believe that the shape of GGNs could be a reliable

CT sign for determining GGNs natures. However, some other studies^[13] have shown that pre-invasive lesions often show round or oval shapes, and benign lesions and IACs are usually irregular in shape. Previous studies^[14] have demonstrated that as the invasion of tumors increases, the proportion of lesions with heterogeneous density also increases. No significant differences in the density uniformity between benign lesions and malignant lesions and significant differences among malignant lesions were observed in our study. However, there was no significant difference in the density uniformity of lesions between the pre-invasive group and MIAs.

In the present study, we showed that margin, internal and surrounding signs were useful CT signs indicating the nature of GGNs. Smooth margins were more common in pre-invasive lesions and MIA, meanwhile invasive adenocarcinomas are more likely to appear as spiculated and lobulated nodules with more bubble signs and air bronchogram. This is because malignant lesions, particularly IAC, the tumor cells inside the nodules grow faster, and the growth rates of different types of cells are different, so the lobulation signs are formed.^[15] The previous literature showed that the bubble sign was one of the important CT imaging signs of lung adenocarcinoma.^[16,17] Its mechanism may be related to tumor growth in the form of lepidic attachment, infiltrating the alveolar wall, and gradually merging into a smaller cavity structure. When internal tumors' fibrous tissue stretches, bubble signs would be more apparent. Our study further confirms the role of the bubble signs in distinguishing benign and malignant GGNs, and also has important value in distinguishing the degree of lesion invasion. Air bronchogram may be caused by aggressive adenocarcinoma due to the aggressive growth of cancer cells and shrinkage of fibrous scars, alveolar collapse, and bronchiolar walls being damaged or stretched, resulting in the deformation and expansion of bronchioles.^[18] This sign is also an important imaging feature to distinguish between benign and malignant lesions. The study by Onoda et al.^[19] found that air bronchogram signs were closely related to lung adenocarcinoma, and could indicate a favorable outcome. As the degree of invasion of malignant lesions deepens, the proportion of air bronchogram signs also increases. However, our study also found that there were no significant differences between pre-invasion lesions and MIAs in air bronchogram. This may be related to the fact that the pre-invasion lesions and MIA are mostly pGGNs, the lesions have less consolidation components and, thus, it is difficult to cause bronchiolar traction.

Fan et al.^[20] studied 82 cases of clinically or pathologically confirmed GGO and found that the pleural indentation sign was an important indicator to diagnose GGO as a malignant tumor. Our study showed that the pleural indentation sign had a considerable significance in distinguishing the benign lesions and malignant lesions of GGNs. The proportion of pleural depression in malignant lesions was significantly higher than that of benign lesions (benign lesions 5.89% vs. malignant lesions 33.96%). In terms of the degree of invasion identification of malignant nodules and prognosis of lung GGNs, pleural indentation signs also have a wide range of applications. Kim et al.^[21] studied 404 cases of subsolid lung nodules and observed that the pleural indentation sign indicated the tumor's visceral pleural invasion and was also a high-risk factor for lung cancer recurrence. Kim et al.^[22] found that the vessel convergence sign could predict the invasion of lung adenocarcinoma with pGGNs and were related to the diameter of the lesions. Our study suggested that vessel convergence in identifying benign and malignant lung GGNs was indeed significant ($p=0.006$, $p<0.05$). In this context, more researches are needed to explore the relationship between them in the future.

Some previous studies have shown that lung adenocarcinomas acting as GGNs are more common in female and more common in the upper lobe of the right lung.^[23] Our study found that neither the benign or malignant nature of GGN, nor the degree of invasion were significantly related to the sex of the patients and the location of the lesions. In terms of smoking history and previous history, patients with malignant or benign GGNs also were no significant differences.

Nonetheless, this study has several limitations. We only included GGNs undergoing surgical resection, which might be considered malignant. This may explain why our study includes a considerably large proportion of invasive adenocarcinomas (51.75%) compared to previous reports.^[24,25] Another limitation is the definition of uniformity of lesion density, which is not widely accepted. The reliability of this definition is subject to further confirmation. In this study, we used manual measurements for the diameters of the GGNs and the diameter of the consolidation component, the results may cause errors. In addition, the sample size of our study was small (particularly for benign lesions), and further research is needed.

In conclusion, the sizes and diameters of consolidation components and mean CT value of GGNs can be used to predict its benign and malignant,

meanwhile the diameters of the consolidation components was a better predictor of the degree of invasion or pathological type than the size. These computed tomography imaging characteristics, including shape, internal and surrounding signs, are helpful to distinguish the benign and malignant lesions and even the degree of invasion. These results were rarely mentioned in past research. From the above, we can draw a conclusion that the comprehensive analysis of computed tomography image characteristics is helpful for the diagnosis of benign and malignant lesions and the differentiation of the degree of invasion of malignant lesions.

Acknowledgments: This study was supported by the Science and Technology funds from Liaoning Education Department (No. LZ2019053).

Ethics Committee Approval: The study was reviewed and approved by the Ethics Committee of the Second Hospital of Dalian Medical University (no: 2021062). The study was conducted in accordance with the principles of the Declaration of Helsinki.

Patient Consent for Publication: A written informed consent was obtained from each patient.

Data Sharing Statement: The data that support the findings of this study are available from the corresponding author upon reasonable request.

Author Contributions: Contributed to the conception of the study: L.C., Z.X., Z.Y.; Contributed significantly to analysis and manuscript preparation: L.C., Z.X., Z.Y., W.C.; Performed the data analyses and wrote the manuscript: Z.Y.; Helped perform the analysis with constructive discussions: W.C., C.X.

Conflict of Interest: The authors declared no conflicts of interest with respect to the authorship and/or publication of this article.

Funding: The authors received no financial support for the research and/or authorship of this article.

REFERENCES

1. Kim HY, Shim YM, Lee KS, Han J, Yi CA, Kim YK. Persistent pulmonary nodular ground-glass opacity at thin-section CT: Histopathologic comparisons. *Radiology* 2007;245:267-75. doi: 10.1148/radiol.2451061682
2. Fang W, Xiang Y, Zhong C, Chen Q. The IASLC/ATS/ERS classification of lung adenocarcinoma—a surgical point of view. *J Thorac Dis* 2014;6(Suppl 5):S552-60.
3. Travis WD, Brambilla E, Nicholson AG, Yatabe Y, Austin JHM, Beasley MB, et al. The 2015 World Health Organization classification of lung tumors: Impact of genetic, clinical and radiologic advances since the 2004 classification. *J Thorac Oncol* 2015;10:1243-60. doi: 10.1097/JTO.0000000000000630
4. Khan T, Usman Y, Abdo T, Chaudry F, Keddissi JI, Youness HA. Diagnosis and management of peripheral lung nodule. *Ann Transl Med* 2019;7:348. doi: 10.21037/atm.2019.03.59

5. Kim HK, Choi YS, Kim K, Shim YM, Jeong SY, Lee KS, et al. Management of ground-glass opacity lesions detected in patients with otherwise operable non-small cell lung cancer. *J Thorac Oncol* 2009;4:1242-6. doi: 10.1097/JTO.0b013e3181b3fee3
6. Furman AM, Dit Yafawi JZ, Soubani AO. An update on the evaluation and management of small pulmonary nodules. *Future Oncol* 2013;9:855-65. doi: 10.2217/fon.13.17
7. Lee HJ, Goo JM, Lee CH, Park CM, Kim KG, Park EA, et al. Predictive CT findings of malignancy in ground-glass nodules on thin-section chest CT: The effects on radiologist performance. *Eur Radiol* 2009;19:552-60. doi: 10.1007/s00330-008-1188-2
8. Ge X, Gao F, Li M, Chen Y, Lü F, Ren Q, et al. Diagnostic value of solid component for lung adenocarcinoma shown as ground-glass nodule on computed tomography. *Zhonghua Yi Xue Za Zhi* 2014;94:1010-3.
9. Shengli Y, Shunliang X, Xiaoping Z, Wenchao H, Jiakang J, Li Y. Differential value of thin-slice CT features of lung mixed ground glass nodules between minimally invasive adenocarcinomas and invasive adenocarcinoma. *Journal of Wezhou Medical University* 2020;50:547-52. doi: 10.1097/MCP.0b013e328354a5f2
10. Godoy MC, Sabloff B, Naidich DP. Subsolid pulmonary nodules: Imaging evaluation and strategic management. *Curr Opin Pulm Med* 2012;18:304-12.
11. Weijie W, Songwei Y, Huixia W, Dongbo L, Jianbo G. Correlation between clinical and imaging features and pathological classification of lung adenocarcinoma with pure ground-glass nodule. *Henan Med Res* 2020;29:583-6.
12. Gao F, Sun Y, Zhang G, Zheng X, Li M, Hua Y. CT characterization of different pathological types of subcentimeter pulmonary ground-glass nodular lesions. *Br J Radiol* 2019;92:20180204. doi: 10.1259/bjr.20180204
13. Yao L, Chenchen H, Guohua F. Correlation between HRCT image features of lung ground-glass nodules and histological type of lung adenocarcinoma. *J Med Imaging* 2020;30:588-92.
14. Jin X, Zhao S, Wu J, Wu C, Chang R, Jing R, et al. Pathological classification and imaging characteristics of early-stage lung adenocarcinoma with pure ground-glass opacity. *Chinese Journal of Radiology* 2014;48:283-7.
15. Liming H. The value of high resolution CT of pulmonary ground glass nodules in differential diagnosis of benign and malignant nodules. *J Imaging Res Med App* 2020;4:157-8.
16. Snoeckx A, Reyntiens P, Carp L, Spinhoven MJ, El Addouli H, Van Hoyweghen A, et al. Diagnostic and clinical features of lung cancer associated with cystic airspaces. *J Thorac Dis* 2019;11:987-1004. doi: 10.21037/jtd.2019.02.91
17. Haider E, Burute N, Harish S, Boylan C. Lung cancer associated with cystic airspaces: Characteristic morphological features on CT in a series of 11 cases. *Clin Imaging* 2019;56:102-7. doi: 10.1016/j.clinimag.2019.02.015
18. Marchiori E, Hochhegger B, Zanetti G. Dilated air bronchogram inside areas of consolidation: A tomographic finding suggestive of pulmonary lymphoma. *Arch Bronconeumol (Engl Ed)* 2019;55:383-4. doi: 10.1016/j.arbr.2018.11.021
19. Onoda H, Kimura T, Tao H, Okabe K, Matsumoto T, Ikeda E. Air bronchogram in pleomorphic carcinoma of the lung is associated with favorable prognosis. *Thorac Cancer* 2018;9:718-25. doi: 10.1111/1759-7714.12638
20. Fan L, Liu SY, Li QC, Yu H, Xiao XS. Multidetector CT features of pulmonary focal ground-glass opacity: Differences between benign and malignant. *Br J Radiol* 2012;85:897-904. doi: 10.1259/bjr/33150223
21. Kim HJ, Cho JY, Lee YJ, Park JS, Cho YJ, Yoon HI, et al. Clinical significance of pleural attachment and indentation of subsolid nodule lung cancer. *Cancer Res Treat* 2019;51:1540-8. doi: 10.4143/crt.2019.057
22. Kim TJ, Goo JM, Lee KW, Park CM, Lee HJ. Clinical, pathological and thin-section CT features of persistent multiple ground-glass opacity nodules: Comparison with solitary ground-glass opacity nodule. *Lung Cancer* 2009;64:171-8. doi: 10.1016/j.lungcan.2008.08.002
23. Lin G, Li H, Kuang J, Tang K, Guo Y, Han A, et al. Acinar-predominant pattern correlates with poorer prognosis in invasive mucinous adenocarcinoma of the lung. *Am J Clin Pathol* 2018;149:373-8. doi: 10.1093/ajcp/axq170
24. Mao Y, Yang D, He J, Krasna MJ. Epidemiology of lung cancer. *Surg Oncol Clin N Am* 2016;25:439-45. doi: 10.1016/j.soc.2016.02.001
25. Marchiori E, Zanetti G, Barreto MM, de Andrade FT, Rodrigues RS. Atypical distribution of small nodules on high resolution CT studies: Patterns and differentials. *Respir Med* 2011;105:1263-7. doi: 10.1016/j.rmed.2011.02.010